and

$$c^*=c_{11}-c_{12}-2c_{44}$$

with

$$\xi_\perp=1.4,\ \eta_\perp=0.67 \text{ and } \zeta_\perp=0.38$$

in the case χ, $H//\langle 111\rangle$; ε is the energy of a hole and V the volume of the crystal. The coefficients $\xi_\perp$, $\eta_\perp$ and $\zeta_\perp$ are anisotropy parameters which depend on the effective mass ratio $m_\perp/m_\parallel$.

The temperature dependence of the linewidth measured under the compression of 1.8×10^3 kg/cm^2 for the cyclotron transition ($n=0\to1, M_j=-\frac{1}{2}$) is shown in Fig. 6 between 1.5 and 4.2°K together with the theoretical line. Since $\varepsilon\propto T^{1/2}$ in thermal equilibrium, one may expect from eq. (4.3) $1/\tau_\perp\propto T^{3/2}$ as in the case for electrons. One finds, however, the linewidth varies approximately linearly with temperature at the frequency of 70.1 GHz, though the temperature dependence becomes somewhat less steep in the case of 35.3 GHz. This result strongly suggests an appreciable contribution of k_H broadening to the line. In fact, it is easy to show that the resonance linewidth varies linearly with temperature if we assume the transition to occur between two parabolic Landau levels with different curvatures.

One is now to analyze the linewidth. For the valence band problem one has to modify Ito's calculation of conductivity[18] by taking the $\Delta\omega(k_H)$ shift into account. In the case $\chi//\langle111\rangle$ and for the transition ($n=0\to1$, $M_j=-\frac{1}{2}$), the relevant conductivity expression is given by

$$\sigma(X,\eta)=\int_0^\infty dE E^{-1/2}\frac{\{(E+\eta)^{-1/2}+2\sum_n(E-n\eta)^{-1/2}\}^{-1}e^{-(E+\alpha E)}}{1+16Y^2[\eta\{E+\eta)^{-1/2}+2\sum_n(E-n\eta)^{-1/2}\}]^{-2}}\ ; \tag{4.4}$$

where

$$Y=(X-\Delta\omega(k_H))\tau\ ,$$

$$X=\omega-\omega_0\ ,$$

$$\Delta\omega(k_H)=\frac{eH}{\hbar^2c}k_H^2\left(2B^2+\frac{1}{9}N^2\right)\Big/\Delta E$$

and

$$\alpha=\frac{2B^2+\frac{1}{9}N^2}{2\left(A+\frac{1}{3}N\right)\left(A-\frac{1}{6}N\right)}\frac{\hbar\omega_0}{\Delta E}$$

with

$$\eta=\frac{\hbar\omega_0}{k_BT},\quad E=\frac{\hbar^2k_H^2}{2m_\parallel k_BT}\ \text{ and }\ \Delta E=2\varepsilon'\ .$$

In this approximation, we have considered the relaxation process only for the $M_j=-\frac{1}{2}$ ladder set without taking the effect of nonparabolicity into account. Since k_BT, $\hbar\omega_c\ll\Delta E$, the phonon-induced transition probability from $M_j=-\frac{1}{2}$ to $M_j=+\frac{1}{2}$ or to $M_j=\pm\frac{3}{2}$ is considered quite small, and higher order terms can also be neglected to calculate the $\Delta\omega(k_H)$ shift. The so-called reduced linewidth X_{half} is given by

$$X_{half}=X_1-X_2=\tau_\perp\Delta\omega \text{ (half-width)}\ . \tag{4.5}$$

Here X_1 and X_2 should satisfy the equation

$$\sigma(X_i,\eta)=\frac{1}{2}\sigma(X_{max},\eta),\ i=1 \text{ and } 2\ . \tag{4.6}$$

By adjusting the theoretical value of X_{half} to be equal to the experimental one at 1.5°K (see Fig. 7), we obtain $D^2=30$ (eV)^2, where $D^2=1.4D_d^{V2}+0.67D_d^VD_{u'}+0.38D_{u'}^2$. The D^2 value obtained here is somewhat smaller than that obtained in the previous work,[19] in which the estimation of $\Delta\omega(k_H)$ as well as employed values of the band parameters were inadequate. For solving eq. (4.4) numerically, the NEAC 2200-500 computer has been used. Figure 8 shows that stress dependence of the linewidth at 1.5°K. We have a nice fit of experimental data with calculation. D_d^V is now obtainable from eq. (4.3), using the values of $D_{u'}$ and D^2. Solution of the quadratic equation yields $D_d^V=-5.2$ or $+3.3$ eV. Choice between these two roots is a difficulty. It should be made not to contradict with experimental results for the variation of the energy gap against hydrostatic volume change. A little more discussion will be made in the next section.

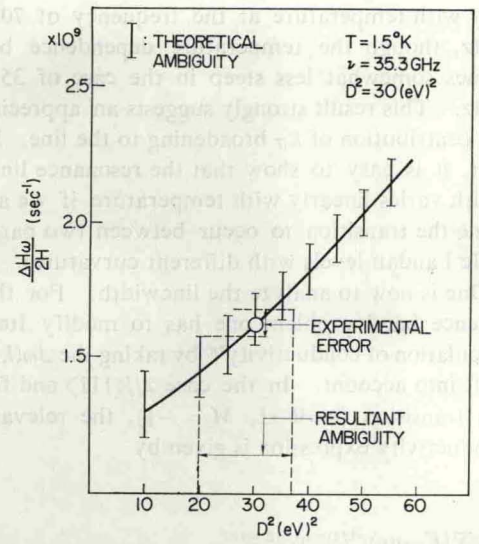

Fig. 7. Dependence of the half-width $\frac{\Delta H\omega}{2H}$ on D^2.
The solid curve refers to the theoretical calculation for χ, $H//\langle 111\rangle$ and 35 GHz at 1.5°K.

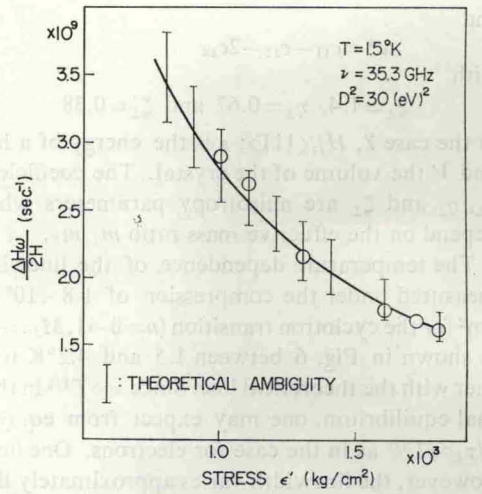

Fig. 8. Stress dependence of half-width of the hole cyclotron transition ($n=0\to1$, $M_j=-\frac{1}{2}$) under the conditions shown.

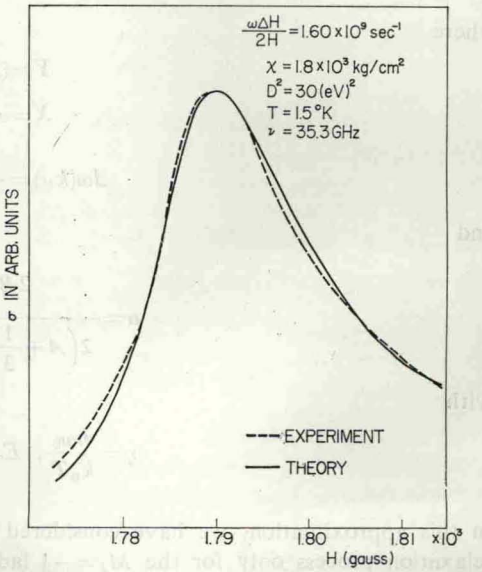

Fig. 9. Theoretical and experimental lineshapes for the transition line ($n=0\to1$, $M_j=-\frac{1}{2}$).

§ 5. Discussions

1) Characters of the quantum lines

For measuring the width of a quantum line, resolution is essential. The condition $|\omega_{c1}-\omega_{c2}|>\Delta\omega$ (we shall call this the secondary condition) is required on top of the ordinary condition for observability of cyclotron resonance; *i.e.*, $\omega_{c1}\tau$ and $\omega_{c2}\tau$ be greater than unity (we may call this the primary condition). Here, ω_{c1} and ω_{c2} are angular frequencies at adjacent peaks, while $\Delta\omega$ the linewidth. In our experiments the maximum value of $|\omega_{c1}-\omega_{c2}|/\Delta\omega$ is 10. In order to get an optimum resolution as well as signal-to-noise ratio, one should control the stress very carefully. At moderate stress, both $|\omega_{c1}-\omega_{c2}|$ and $\Delta\omega$ are nearly inversely proportional to the stress (see Fig. 5(a) and Fig. 8). At high stress, dependence of the former on stress does not change, while the latter approaches a limiting value. The resolution of lines then becomes worse as the stress is increased. The fact that we cannot observe the higher quantum lines with enough resolution is explained by the reason that $\Delta\omega$ gets larger as the quantum number is increased and thereby the secondary condition is no longer satisfied. This is because the higher energy levels are more strongly coupled with the bands $M_j=\pm\frac{3}{2}$.

The lineshape of a quantum line differs from the usual Lorentzian shape. Because of the $\Delta\omega(k_H)$ contribution, it has an asymmetric structure as is characterized by a shoulder on the high magnetic field side. One can see this feature in eq. (4.4) and Fig. 9.

In Fig. 3, quantum lines are distinct up to fairly high n values. Though the higher states have smaller populations, the oscillator strength which is proportional to $(n+1)$ makes up for that.

2) Inverse mass parameters A, B, N, g-factor (2κ) and shear deformation potential constants D_u and $D_{u'}$

The values of the inverse mass parameters A, B, and N as well as those of the shear deformation potential constants D_u and $D_{u'}$ can be deter-